PARTICLE IMAGE VELOCIMETRY AND THERMOMETRY IN FREEZING WATER

T. A. Kowalewski, A. Cybulski, M. Rebow

Keywords: *natural convection, freezing, liquid crystals, particle image velocimetry and thermometry*

Abstract

A new experimental technique based on computational analysis of the colour and displacement of thermochromic liquid crystal tracers is applied to determine both the temperature and velocity fields of natural convection in freezing water. It combines Particle Image Thermometry and Particle Image Velocimetry. Full 2-D temperature and velocity fields are determined from two or more colour images taken for the selected cross-section of the flow.

1 Introduction

Properties of crystals, metals or alloys made by solidification processes are, to a large degree, determined by natural convection. Numerical modelling of this moving boundary, strongly non-linear, thermal flow problem is not a trivial task. Complex flow structures and their sensitivity to small variation of the flow parameters and boundary conditions necessitate application of appropriate experimental methods to validate the numerical results [1]. This requires application of full field acquisition methods, which can give transient data for velocity and temperature fields, reliable enough for their subsequent comparison to the CFD models.

The proposed method is based on an application of Thermochromic Liquid Crystal (TLC) suspended in a working fluid as seeding. Digital Particle Image Velocimetry (DPIV) combined with digital colour analysis (DPIT) allow simultaneous measurement of 2-D velocity and temperature flow fields. Collected transient data for the temperature and velocity fields as well as the interface position can be directly compared with numerical calculations. In the following we present our attempts to implement the DPIV & T for studying natural convection with phase change. Investigations are performed for freezing water in two configurations: in a differentially heated cavity, and in a lid cooled cavity. The experimental results gained are compared with numerical simulations performed using the modified 3-D finite difference code ICE3D [2].

Author(s): *T. A. Kowalewski[1], A. Cybulski[1], M Rebow[2]*

[1]Polish Academy of Sciences, IPPT PAN, Swietokrzyska 21, PL 00-049 Warszawa.
[2]Warsaw University of Technology, ITC-PW, Nowowiejska 25, PL 00-665 Warszawa
Website: http://www.ippt.gov.pl/~tkowale/

2 Formulation of the problem

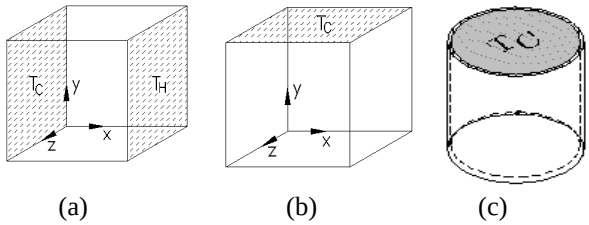

(a) (b) (c)

Fig. 1 Differentially heated (a) and lid cooled cube (b), lid cooled cylindrical cavity (c).

We consider convective flow of water in a cube of 38mm internal size and in a

cylindrical cavity of 37mm internal diameter and 41mm height (Fig. 1). Two flow configurations are considered. In the first, natural convection develops in the differentially heated cube surrounded by air (Fig. 1a). Two opposite walls made of black anodised metal are assumed to be isothermal. One of them is held at temperature T_h= 10^{o}C, the opposite wall is held at temperature T_c= -10^{o}C. The other four walls, made of Plexiglas, are nominally insulators of finite thermal diffusivity. In the second configuration (Fig1b,c), the top metal wall of the cavity is isothermal at low temperature T_c. The other walls are non-adiabatic, allowing a heat flux from the external water bath kept at the temperature T_h. Due to forced convection in the bath it can be assumed that the temperature at the external surfaces of the box is close to the bath temperature. The temperature field at the inner surfaces of the walls adjusts itself depending on both the flow inside the box and the heat flux through and along the walls. To some extent this configuration resembles directional solidification in a Bridgman furnace used for crystal growth. Effects of heat flux through the side walls (Plexiglas versus glass walls), and geometry (cube cavity and vertical cylinder), on the flow structure and its stability are investigated.

3 Experimental apparatus and procedure

A sketch of the experimental apparatus is shown in Fig. 2. It consists of a convection box, a halogen tube lamp, a 3CCD colour camera (KYF55 JVC) and a 32-bit PCI-bus frame grabber (AM-CLR Imaging Tech. Inc.). The flow field is illuminated with a 2mm thick sheet of white light from a specially constructed halogen lamp, and observed in the perpendicular direction. The 24-bit colour images of 768x564 pixels have been acquired using a 64MB Pentium 133 computer.

The temperature of the isothermal walls and that of the water in the bath (eventually surrounding the cavity) are controlled by thermostats. The computer controlled system of three stepping motors allows the acquisition of images of several cross-sections, both for horizontal and vertical planes, fully automatically within several seconds. This allows three-dimensional analysis of the whole flow domain. The computer also controls switching of the halogen lamp and records readings from four control thermocouples and the thermostats.

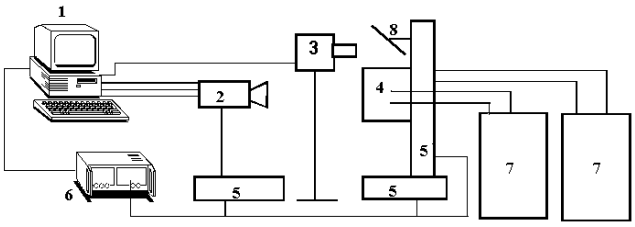

Fig.2. Schematic of the experimental system. PC (1) with the acquisition card controls: camera (2), halogen lamp (3) and three stepping motors (5) through driver (6). Temperature in the cavity (4) controlled by two thermostats (7). Mirror (8) used to direct light sheet.

The experiment starts when the inlet valves are abruptly opened to the coolant passages. Distilled water has been selected as flow media for its relatively well known thermophysical properties. A fine dispersion of raw liquid crystal material was used as tracers. Their mean diameter is about 50μm.

3.1 Liquid Crystal Thermography

TLC temperature visualization is based on the property of some cholesteric and chiral-nematic liquid crystal materials to reflect definite colours at specific temperatures and viewing angle. The colour change for the TLC ranges from clear at ambient temperature, through red as temperature increases and then to yellow, green, blue, and finally clear again at the highest temperature. These colour changes are repeatable and reversible as long as the TLCs are not physically or chemically damaged.

TLCs are widely used to map temperature distributions on surfaces [3]. Application of TLC tracers to flow problems [4], combined with digital image analysis gave impact to quantitative and fully

automatic temperature and velocity evaluation, based on DPIV [5] and DPIT [6]. In the present study use of both digital evaluation techniques, as initiated by Hiller et al. [7], allows us simultaneous and fully automatic measurements of temperature and velocity fields for selected 2-D flow cross-section.

The temperature measurements are based on a digital colour analysis of *RGB* images of the TLCs seeded flow field. For evaluating the temperature the *HSI* representation of the *RGB* colour space is used. The incoming *RGB* signals are transformed pixel by pixel into *Hue, Saturation and Intensity*. Temperature is determined by relating the hue to a temperature calibration function [8,9]. Application of the PIV&T method for the freezing problem yields several additional experimental constrains. The investigated temperature range is well defined by the phase change temperature. Hence the colour-play properties of the TLC material have to be correctly matched. In addition, the ice surface generates additional light scattering and reflections. These may generate unexpected colour shifts or/and image distortions in regions adjoining the phase front, and have to be accounted for throughout the calibration procedure.

Comparing to surface thermography, the use of TLC as dilute suspension in a fluid bears additional problems. First of all the colour images of the flow are discrete, i.e. they represent a non-continuous mist of points. Secondly, due to the secondary light scattering, its reflections from the side walls and internal cavity elements, the overall colour response may be distorted. Hence, the use of specially developed averaging, smoothing and interpolating techniques are indispensable to remove ambiguity in the resulting isotherms. Further, every experimental set-up needs its own calibration curve obtained from the images taken for the same fluid, at the same illumination, acquisition and evaluation conditions.

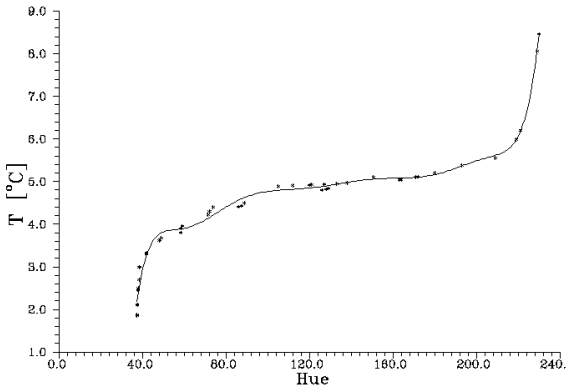

Fig. 3. Temperature vs. Hue for TLC sample TM-MIXC. Calibration curve obtained by 8th order polynomial fitted to the experimental points.

Our 8-bit representation of the hue value assures resolution better than 1%. However, the colour - temperature relationship is strongly non-linear (Fig. 3). Hence, the accuracy of the measured temperature depends on the colour (hue) value, and varies from 3% to 10% of the full colour play range. For the TLC used (TM from Merck) it results in an absolute accuracy of 0.15°C for lower temperatures (red-green colour range) and 0.5°C for higher temperatures (blue colour range). The most sensitive region is the colour transition from red to green and takes place for a temperature variation of less then one degree Celsius. To improve the accuracy of temperature measurements, some experiments have been repeated using four different types of TLC, so that their combined colour play sensitivity range covered temperatures from -5°C to 14°C.

The colour of light refracted by TLCs also depends on the observation angle. Our previous investigations [10] have shown that this relation is linear with the slope equal to 0.07°C per 10° change of the angle. Therefore, it is important that the angle between the illuminated plane (light sheet plane) and the camera is fixed and that the viewing angle of the lens is small. In the present experiment the flow is observed at 90° using a 50mm lens and 1/3' sensor, i.e. the camera viewing angle is smaller than 4°.

3.2 Particle Image Velocimetry

The 2-D velocity vector distribution has been measured by digital particle image velocimetry (DPIV). By this method, the motion of the scattering particles, observed in the plane of the illuminating light sheet, is analysed. For this purpose, the colour images of TLC tracers are transformed to B&W intensity images. After applying special filtering techniques [9] bright images of the tracers, well suited for DPIV, are obtained. The magnitude and direction of the velocity vectors are determined using an FFT-based cross-correlation analysis between small sections (interrogation windows) of one pair of images taken at the given time interval. The spatial resolution of the method is limited by the minimum amount of tracers present in the interrogation window. In practice, the minimum window size was 32x32 pixels. On the other hand, the dimension of the interrogation window limits the maximum detectable displacement. Hence, to improve the accuracy and dynamics of the velocity measurements short sequences of images have been taken at every time step. The cross-correlation analysis performed between different images of the sequence (time interval between pairs changes), allows us to preserve similar accuracy for both the low and high velocity flow regions. For some experimental data, the recently developed [11] ODP-PIV method of image analysis has been also used to obtain dense velocity fields. The accuracy of the FFT-based DPIV and that of the ODP-PIV method is 0.6 pixels and 0.15 pixels, respectively. It means that for typical displacement vector of 10 pixels the relative accuracy of the velocity measurement (for single point) is better than 6%.

4 Selected Results

4.1 Differentially heated cavity

This flow configuration resembles a popular "bench mark" case, natural convection in a cubical cavity with differentially heated end walls. However, the behaviour of natural convection of water in the vicinity of the freezing point creates interesting and also difficult for numerical modelling flow structures [12]. The competing effects of positive and negative buoyancy force result in a flow with two distinct circulations (Fig. 4). First one, "normal" clockwise circulation, where the water density decreases with temperature (upper-left cavity region) and an "abnormal" one with the opposite density variation and counter-clockwise rotation (lower-right region). The convective heat transfer from the hot wall is limited by the abnormal circulation, separating it form the freezing front. Hence, the phase front which is only initially flat, with time becomes strongly deformed, with a characteristic "belly" at its lower part. This type of the flow structure appears very sensitive to thermal boundary conditions at the side walls. Despite improvements of the numerical model (side walls are included in the computational domain) [12], the computational results differ in detail from their experimental counterparts (Fig 4d).

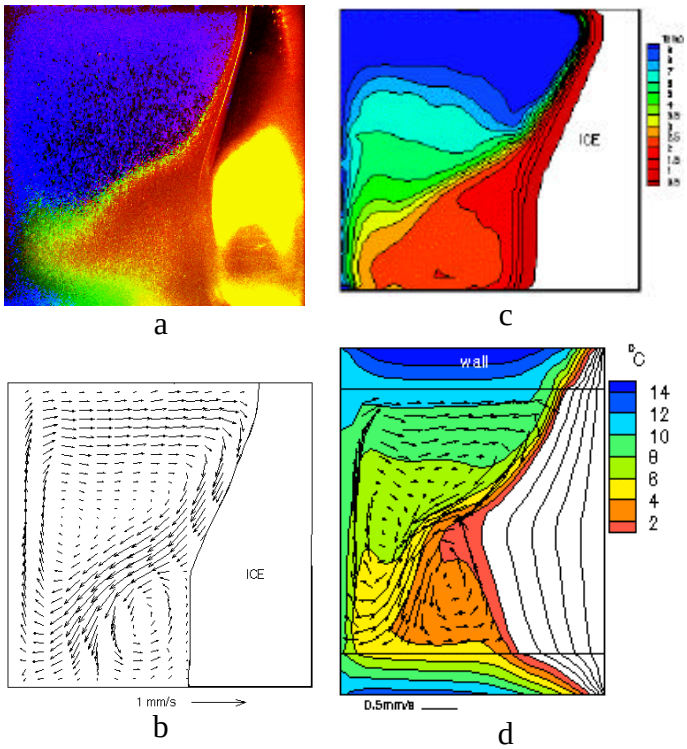

Fig. 4. Ice front observed at centre plane (z=0.5) of the cube at 3000s, T_h=10°C, T_c=-10°C. TLC tracers (a), evaluated velocity (b) and temperature (c) fields. Numerical result (d), the full temperature field solution (with the side walls), external temperature of air 25°C.

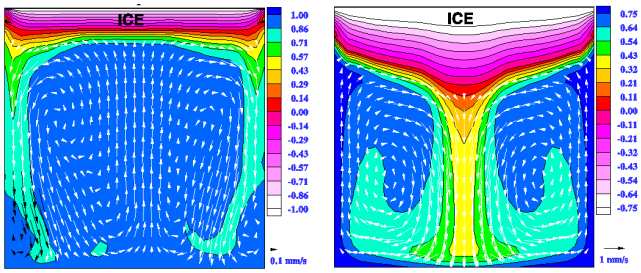

a b

Fig. 5. Onset of convection in the lid-cooled glass cavity; T_h=10°C, T_c=-10°C. Velocity vectors and non-dimensional temperature at the vertical centre plane z=0.5. Numerical simulation for time = 100s (a), and 1000s (b) after cooling starts.

Movies: Ice front observed in differentially heated cavity during 3000s period. Initial supercooling of water visible. *T_h=10°C, T_c=-10°C.* Temperature visualized by TLC tracers (comp. Fig. 4).

An eventual source of observed discrepancies could be supercooling of water, which delays creation of the first ice layer and deforms the flow pattern at the top of the cavity. It is well known that pure water may supercool as far as -40°C, before freezing occurs [13]. Movie 1 shows sequences of the flow images taken during 3000s of the freezing experiment. Initially the whole cavity and fluid is at hot wall temperature T_h. The experiment starts by abruptly dropping the cold wall temperature to -10°C. At the first moment a red plume of water at temperature well below freezing point moves along the cold wall to the top of the cavity (red colour of TLC indicates cold liquid). It may cover as much as 30% of the upper wall before sudden solidification occurs (usually after 30-100s). An ice layer developed at the top quickly melts due to the hot clockwise circulation, but initial disturbance of the flow and temperature fields may affect the front propagation for a longer period.

4.2 Lid cooled cavity

The onset of convection and the stability of an initially isothermal fluid in a cubical box instantaneously cooled from above have been extensively investigated for water, both with and without phase change. Physically this configuration bears some similarity to the Rayleigh-Bénard problem. However, due to altered thermal boundary conditions at the side walls, the flow structure is different. The cubic symmetry of the box imposes a strong downward flow along the vertical axis of symmetry. Before a stable final flow structure is achieved, several oscillatory changes in its pattern are observed. The initial flow instabilities, well seen in the TLCs visualized temperature field, are also reproduced in the numerical simulations. Figure 5 shows numerical simulation of the transient flow development for the glass cavity. Initial temperature of the cavity and fluid is equal T_h=10°C, then the lid temperature is abruptly decreased to T_c = –10°C. The flow starts, when an initial cold thermal boundary layer at the lid becomes unstable, breaking down to four symmetrical plumes falling down along the side walls. This in turn generates several recirculating zones, transporting heat and vorticity from the side walls to the centre. Within 3-5 minutes a general flow pattern is established. In the centre plane two “jets” of cold liquid are streaming along the side walls, and another along axis of symmetry of the box (Fig. 5a). This configuration is unstable. Depending on experimental disturbances or numerical noise present, after 4-8 minutes a dramatic flow pattern

transformation takes place. Passing through several strongly asymmetrical flow forms, a final configuration with a single cold jet along the cavity axis and a reverse flow along side walls are established (Fig. 5b). The final state is reached after about 40 minutes.

It was found that the creation of the ice layer at the lid has a stabilizing effect on the flow. The grooving of the ice-fluid interface which formed on the lid of the cavity imposed the direction and character of the flow, damping the instabilities observed for the pure convection case. There is also a density inversion under the lid which decelerates the main jet and limits the strong generation of vorticity in that region.

Due to the stochastic development of the flow pattern, direct comparison of transient experimental and numerical results becomes difficult at early time steps. Hence, to minimise uncertainty of the initial conditions, the second set of investigations is performed. In this case, we call it the "warm start", the freezing starts after a steady convection pattern is established in the cavity. This initial flow state corresponds to natural convection without phase change, with the lid temperature set to 0^{o}C.

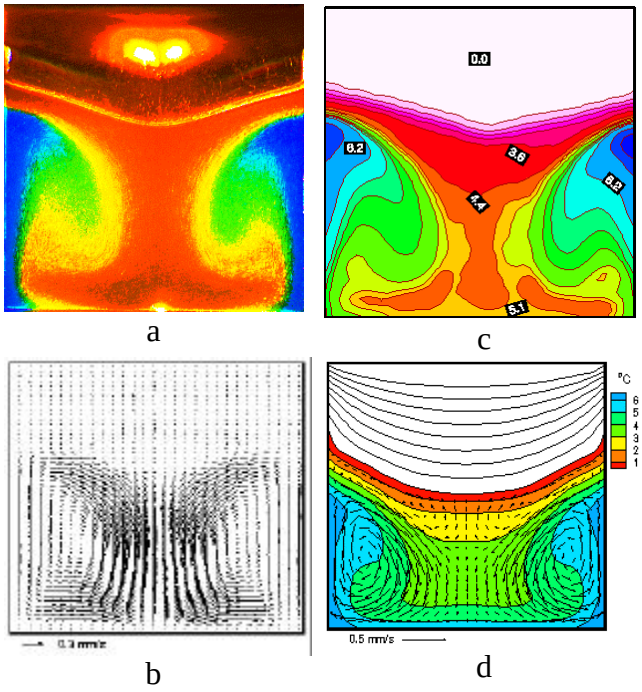

Fig. 6. Ice front observed at 3600s after "warm start", centre plane of lid cooled Plexiglas box; T_h=20°C, T_c=-10°C. TLC tracers (a), evaluated velocity (b) and temperature (c) fields, (d)- numerical solution.

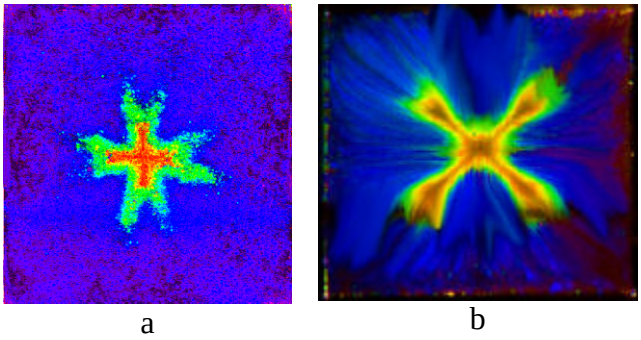

Fig. 7. TLC visualised temperature distribution directly under cooled lid for cubic box of 8mm Plexiglas walls (a) and 2mm glass walls (b).

Movie 2 displays experimental result of the freezing process which starts from the developed natural convection. Regular flow pattern is seen, with the central, stable cold jet at the cavity axis. Figure 6 shows the temperature and velocity field evaluated for the time step 3600s, and compared with its numerical counterpart. Difficulties in achieving quantitative agreement are evident. One of the possible agents is difference in the three-dimensional flow structure.

The flow visualisation performed in the lid cooled cavity shows the existence of a

Movie: Ice front in lid cooled cavity observed during 3600s, freezing starts from developed convection flow ("warm start"). Plexiglas cavity, T_h=20°C, T_c=-10°C (comp. Fig. 6).

complex spiralling structure transporting fluid up along the side walls and down in a central cold jet along the cavity axis [1]. For walls of high heat conductivity (glass), eight symmetric cells are created by the flow. For Plexiglas walls additional small recirculation regions appear, separating the main cells. This is also manifested in the complex structure of the ice surface. Both in the computed and observed ice surface, a star-like grooving reflects eight-fold symmetry of the flow. A colour play of TLC seeded flow images taken directly under the lid (Fig. 7a, b) recoils differences of flow structures in the temperature pattern. It appears, that only a slight change of the *thermal boundary conditions* at the side walls may modify the flow pattern. This was observed by replacing the side walls of low conductivity Plexiglas with thin glass walls.

A numerical simulation of the flow, using simple, heat flux based thermal boundary conditions at the side walls, has shown discrepancies. Although the computational results confirmed the eight-fold symmetry of the temperature and flow fields observed experimentally, their orientation was different. Moreover, the measured isotherms were evidently shifted to higher values. Quantitative differences were noticed for the temperature distribution observed at the horizontal cross-section [14]. It was found that heat flux through, as well as along the walls has to be incorporated to the numerical model. Inclusion of the side walls in the computational domain and solving the coupled fluid-solid heat conduction problem improved the agreement with the observed flow pattern. Also the observed temperature distribution as well as its symmetry were fully recovered in the numerical results [15]. It was only as a result of use of *both* the experimental and numerical methods that the fine structures of the thermal flow were fully understood.

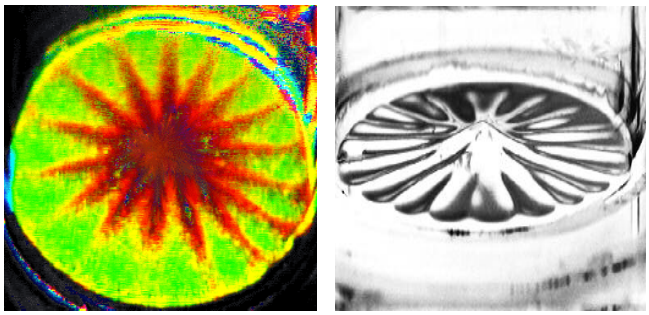

a b

Fig. 8. TLC visualised temperature distribution under cooled lid for cylindrical cavity (a), ice structure appearing under the lid.

An interesting example of the temperature pattern observed for the cylindrical cavity is shown (Fig. 8a). Despite the cylindrical symmetry, azimuthal flow structures appear, dividing the flow domain into a regular sequence of 16-18 radial running rolls. Experimental evidence of this flow symmetry breaking was only possible with help of the TLC visualisation method. It is interesting to note that these structures remain when the phase change takes place. Figure 8b shows characteristic star-like grooves in the ice surface growing at the lid.

5. Conclusions

The simultaneous measurement of flow and temperature fields using TLCs allowed a quantitative experimental description of the onset of convection combined with freezing of water. The full field experimental data of the flow appeared to be very valuable for further improvements and modifications of the numerical code. The comparison of experimental data with their numerical counterparts helped us to encounter several differences in details. It seems, that to improve modelling the influence of such effects as supercooling, the thermal boundary layer at the ice surface, non-homogeneous ice structure and heat conduction contact resistance at ice-wall surfaces, have to be still investigated.

Acknowledgements

The authors are indebted to G. Yeoh, G. de Vahl Davis and E. Leonardi (UNSW) for their computer code FREEZE3D [2]. This work was supported by the Polish Scientific Committee (KBN Grant No. 3T09C00212).

References

[1] Kowalewski TA. Experimental validation of numerical codes in thermally driven flows. *Adv. in Computational Heat Transfer CHT-97, Cesme*, Begell House, pp.1-15

[2] Yeoh GH. Natural convection in a solidifying liquid. *Ph.D. Thesis*, University of New South Wales, 1993.

[3] Hay JK, Hollingsworth DK. A comparison of trichromic systems for use in the calibration of polymer-dispersed thermochromic liquid crystals. *Exp. Thermal Fluid Scs*, Vol. 12, pp.1-12,1996.

[4] Hiller W, Kowalewski TA. Simultaneous measurement of the temperature and velocity fields in thermal convective flows. *Flow Visualization IV*, Paris, pp. 617-622, Hemisphere, 1987.

[5] Westerweel J. *Digital Particle Image Velocimetry - Theory and Application*. Delft University Press, 1993.

[6] Dabiri D, Gharib M. Digital particle image thermometry: The method and implementation. *Exp. in Fluids*, Vol. 97, pp.77-86, 1991.

[7] Hiller WJ, Koch St, Kowalewski TA, Stella F. Onset of natural convection in a cube. *Int. J. Heat Mass Transfer*, Vol. 36, pp.3251-3263, 1993.

[8] Kowalewski TA, Cybulski A. Experimental and numerical investigations of natural convection in freezing water. *Int. Conf. on Heat Transfer with Change of Phase*, Kielce, *Mechanics*, Vol. 61/2, pp.7-16, 1996.

[9] Kowalewski TA, Cybulski A. Natural convection with phase change (in polish). *IPPT Reports* 8/97, IPPT PAN, 1997.

[10] Hiller WJ, Koch St, Kowalewski TA. Simultane Erfassung von Temperatur- und Geschwindigkeitsfeldern in einer thermischen Konvektionsströmung mit ungekapselten Flüssigkristalltracern. *2D-Meßtechnik DGLR-Workshop*, Markdorf, DGLR-Bericht 88-04, pp.31-39, 1988.

[11] Quénot G, Pakleza J, Kowalewski TA. Particle Image Velocimetry with Optical Flow. *Exp. in Fluids, Vol.25, pp.177-189, 1998.*

[12] Kowalewski TA, Rebow M. Freezing of water in the differentially heated cubic cavity. *Int. J. CFD* (submitted).

[13] Knight CA. *The freezing of supercooled liquids*. D. Van Nostrand Co., 1967.

[14] Abegg C, de Vahl Davis G, Hiller WJ, Koch St, Kowalewski TA, Leonardi E, Yeoh GH. Experimental and numerical study of three-dimensional natural convection and freezing in water. *Proc. of 10th Int. Heat Transfer Conf.*, Brighton, Vol. 4, pp 1-6, 1994.

[15] Söller C, Hiller WJ, Kowalewski TA, Leonardi E. Experimental and numerical investigation of convection in lid cooled cavities - effects of non-ideal thermal boundary conditions on three-dimensional flow. *3rd ICIAM Congress*, Hamburg, 1995.